GA–A23981

INFRARED MONITORING OF 110 GHz GYROTRON WINDOWS AT DIII–D

by
Y. GORELOV, J. LOHR, R.W. CALLIS,
and D. PONCE

MAY 2002

DISCLAIMER

GA–A23981

INFRARED MONITORING OF 110 GHz GYROTRON WINDOWS AT DIII–D

by
Y. GORELOV, J. LOHR, R.W. CALLIS,
and D. PONCE

This is a preprint of a paper presented at the 12th Joint Workshop on Electron Cyclotron Emission and Electron Cyclotron Resonance Heating, May 13–16, 2002, in Aix-en-Provence, France, and to be published in the *Proceedings.*

Work supported by
the U.S. Department of Energy
under Contract DE-AC03-99ER54463

GA PROJECT 30033
MAY 2002

INFRARED MONITORING OF 110 GHz GYROTRON WINDOWS AT DIII–D

Y. GORELOV, J. LOHR, R.W. CALLIS, D. PONCE

General Atomics, P.O. Box 85608, San Diego, California 92186-5608

The combination of low millimeter wave losses and excellent thermal conductivity with good mechanical properties make artificial chemical vapor deposition (CVD) diamonds a compelling choice for 1 MW 110 GHz gyrotron windows. Five gyrotrons are currently operating at the DIII–D tokamak. Three Gycom gyrotrons have boron nitride (BN) ceramic windows. Due to temperature increases of the windows up to about 930°C, the pulse duration of these tubes is limited to 2 s for output power near 800 kW. Two Communications and Power Industries (CPI) gyrotrons with diamond windows are also installed and operating. The diamond disks of these windows and the construction of their water-cooling assemblies are different. This paper reviews the infrared (IR) measurements of both types of gyrotron windows, with emphasis on the two diamond designs.

1. Introduction

Electron cyclotron resonance heating (ECRH) and current drive (ECCD) are important areas of scientific exploration in studies of plasmas for thermonuclear fusion energy research. Gyrotron tubes producing nearly 1 MW for ECRH at the tokamak second harmonic electron cyclotron resonance are available at present. At the General Atomics DIII–D tokamak project, there are five gyrotrons at a frequency of 110 GHz with nearly 1 MW output power per unit, which are currently installed and operating. Maximum pulse length of the Gycom[1] gyrotrons is limited to 2 s due to heating of the boron nitride windows. Two CPI[2] gyrotrons have diamond windows that theoretically introduce the possibility for continuous wave (cw) mm-wave high power gyrotron operation.

2. Performance of BN windows

Absorption of the 110 GHz rf power in the BN windows on the Gycom gyrotrons ranges from 3% to 4% of the total output power. This means that, during the rf pulse, the window disks absorb up to 32 kW, producing a rapid increase in the window temperature. In order to reduce the peak power density at the window, the Gycom tubes were designed to produce non-Gaussian rf beams with the power filling the window aperture as uniformly as possible. In Fig. 1(a), the infrared image of the rf beam close to the window surface for one of these tubes is shown.

In order to couple these broadened rf beams into the 31.75 mm diameter circular waveguide in the DIII–D installation, a pair of phase correcting and focusing mirrors are used. Despite the phase correction, the conversion to a Gaussian beam has relatively poor efficiency and up to 18% of the generated power is lost. This power appears as heat absorbed in the chamber containing the mirrors. As indicated in Fig. 2, the maximum temperature of the BN windows reaches about 900°C during a 2 s pulse at 800 kW.

3. Performance of CVD diamond windows

Two CPI 110 GHz gyrotrons with diamond windows have been installed at DIII–D. The windows differ in thickness and in the design of the water cooling edge interface. The main parameters of the two windows are summarized in Table 1. In Fig. 1(b), an infrared image of

[1]Gycom, 46 Ulyanov Street, Nizhny Novgorod, Russia.
[2]Communications and Power Industries, 831 Hansen Way, Palo Alto California, USA.

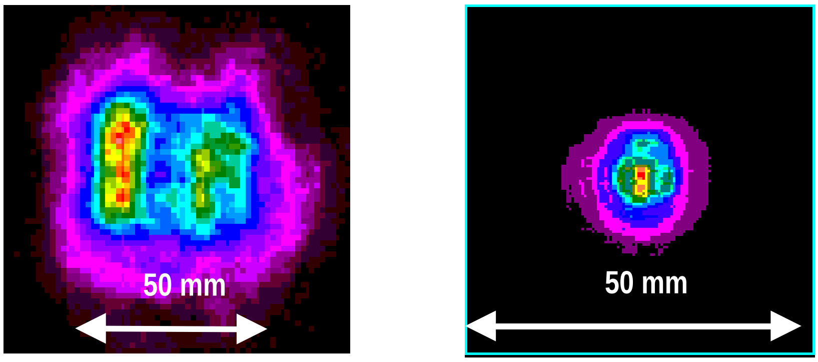

Fig. 1. IR images of Gycom BN and CPI diamond windows heated by transmission of high power rf beams. The rf beam in Fig. 1(a) was intentionally broadened to reduce the peak power loading. This was not required for the CVD diamond window in Fig. 1(b).

Table1. Design and Performance Parameters for the Diamond Windows on the Two CPI VGT-8110 Gyrotrons in Service at DIII–D

Gyrotron name	Window clear aperture	Disk outside diameter	Window thickness	Thermal conductivity	tan(δ)	P_{abs} at 800 kW
CPI-P2	50.8 mm	57.0 mm	1.14 mm	6.5 kW/m^2K	$\leq 2\times10^{-4}$	1.8 kW
CPI-P3	50.8 mm	73.5 mm	1.71 mm	6.5 kW/m^2K	$\leq 5\times10^{-5}$	2.0 kW

the Gaussian rf beam produced by one of these gyrotrons is presented for comparison with the broadened beam from the gyrotrons with BN windows. Despite the peaked Gaussian beam, the maximum allowable power density is not exceeded for the diamond windows because of extremely low loss and high thermal conductivity.

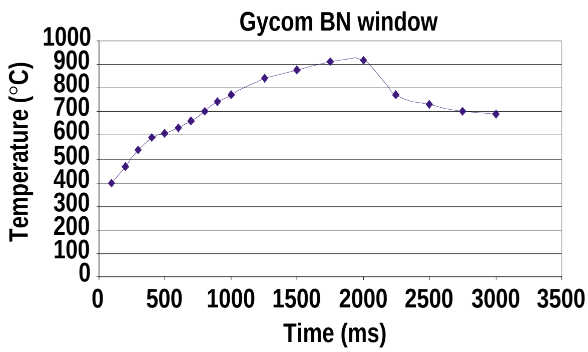

Fig. 2. Time dependence of maximum BN temperature during 2 s rf pulse at about 800 kW generated power. Window heating determines the maximum pulse duration of gyrotrons with BN ceramic windows.

To evaluate the temperature of a diamond disk from IR measurements, several factors have to be taken into account. First, the emissivity of the diamond disk itself in the range of the IR camera sensitivity (3–5 μm) is low and depends on the temperature. Second, the waveguide transmission line and coupling system are evacuated, so the window must be viewed off-axis through a sapphire viewport in the matching optics unit (MOU). The window is partly transparent for IR radiation from inside the gyrotron. Radiation from this source also will contribute to the final IR image and will bias the temperature determination. The peak temperature of the CPI-P2 diamond window, determined from infrared data corrected for the view and the emissivity as noted above, is shown in Fig. 3. The figure shows high time resolution data for a 2.0 s long 850 kW pulse and lower resolution data on the same window for a 5.0 s 650 kW pulse. The temperature equilibrates after about 2.5 s with a peak value of about 160°C, which is in agreement with ANSYS modeling. The safety factor below the yield stress of 350 MPa is more than three.

The oscillations superimposed on the 2 s pulse data are at 4 Hz, which is the frequency of the collector sweep coil. As the electron beam heats the collector at different places, radiation from the interior is detected as part of the infrared signature. The amplitude of these oscillations, about ±5°C, indicates the range of error introduced by the contribution to the image from inside the gyrotron.

The uncorrected infrared images of the windows on the CPI-P2 and CPI-P3 gyrotrons differ qualitatively. In Fig. 4(a) the CPI-P2 window is seen to have a Gaussian character with several pinpoint hot spots. The image in Fig. 4(b) is of the CPI-P3 window and has a much broader temperature profile, which is nearly flat across the central part of the image. The images were obtained under similar conditions at the end of 5.0 s long pulses at about 800 kW transmitted power. Correction for the factors noted above did not change the qualitative differences between the images.

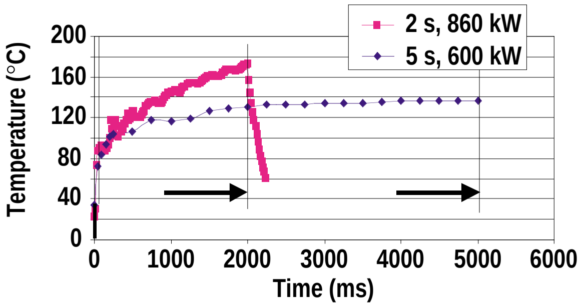

Fig. 3. Time dependence of the peak temperature of a CVD diamond window transmitting 860 kW and a 5.0 s pulse at lower power and lower time resolution oscillations in the 2.0 s data have a frequency of 4 Hz, which exactly coincides with the frequency of the collector sweep coil. The rf signals have no such oscillations, so we have drawn the conclusion that IR emission from the collector of the gyrotron is seen by the IR camera. The ±5°C amplitude of the oscillations indicates the error introduced from this source.

After correction for the viewing geometry and subtraction of the background radiation from inside the gyrotron, the temperature profile for the CPI-P2 window has a Gaussian shape which agrees fairly well with a modeling calculation for 1 MW transmitted power. Figure 5 compares the measured and calculated profiles. The profile of the CPI-P3 temperature after the same corrections is shown in Fig. 6. The analysis cut was intentionally taken to cross several of the hot spots, but the fundamental conclusion that the profiles are quite different remains. The hot spots will be discussed below. The qualitative differences between the two profiles cannot be explained by the fact that CPI-P3's window is 50% thicker than CPI-P2's, but may arise from the very different cooling geometries for the CPI-P2 and CPI-P3 windows.

Concern about the efficiency of radial heat transfer to the cooling water in the CPI-P2 design led to a modification in the design for the CPI-P3 window. The two geometries are compared in Fig. 7. In the CPI-P2 window, only the outer circumference of the disk is in direct contact with the cooling water. For CPI-P3, however, the disk was extended into the cooling flow, greatly increasing the heat transfer efficiency. This, plus a higher thermal conductivity for the CPI-P3 window, could explain the flatter profile. Additional ANSYS calculations are being performed to determine whether thermal conductivity alone could account for the differences between the two measurements.

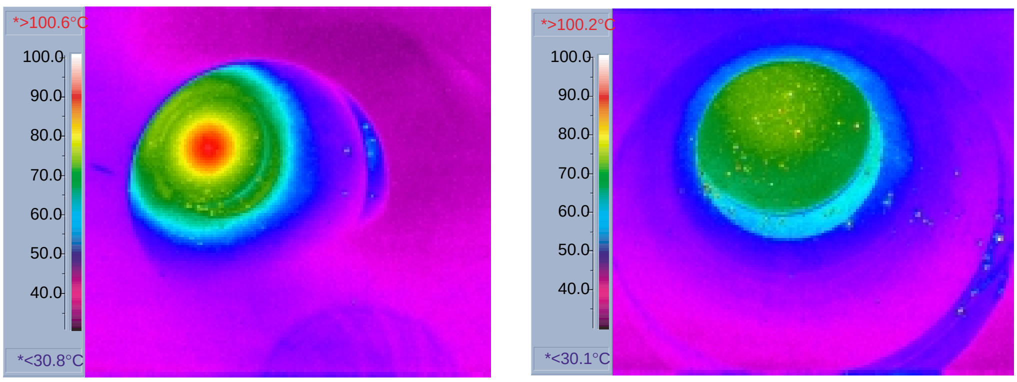

Fig. 4. Infrared images of Tinman, 4(a), and CPI-P3,4(b), diamond windows after 5 s rf pulses. Both windows show apparent hot spots, which could be regions of higher emissivity or actual hotter regions due to contamination. The temperature profiles are qualitatively different for the two windows.

Infrared monitoring has made it possible to detect local hot spots on diamond windows. Roman scattering confirmed that some of these spots were due to graphite contamination on the surface of the disk. Although the total number of local hot spots decreased after surface cleaning by grit blasting of a window already mounted on a gyrotron, some of these spots remained. All these IR results from the CPI-P2 gyrotron were considered during

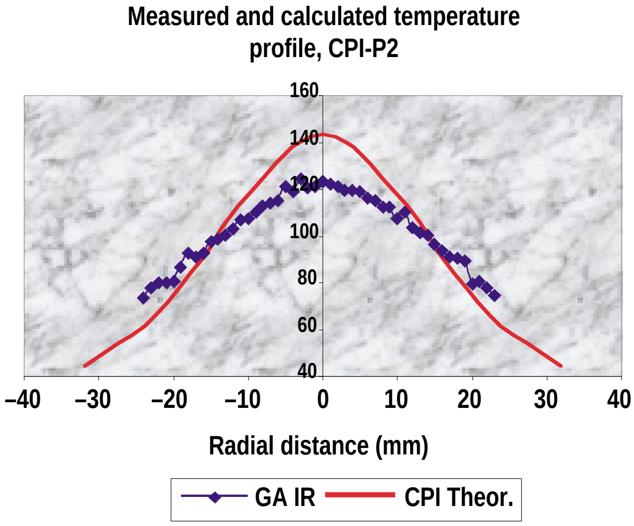

Fig. 5. The uncorrected temperature profile for CPI-P2's window is centrally peaked with a central value about 30°C above the edge. Corrections for the view and background radiation increase this difference to about 80°C. The corrected profile is plotted.

manufacturing of CPI-P3, the next gyrotron in the series. Special precautions were taken to prevent any contamination on the surface of the diamond disk. Despite these precautions, initial IR measurements of the CPI-P3 diamond window indicated the presence of some hot spots. Additional blowing by dry nitrogen gas did not decrease the number of hot spots, so it is unlikely that these spots are some dust on the diamond surface. It is known that in CVD diamond there is often a significant density of cracks and voids along grain boundaries. These micro-features in the diamond with non-diamond carbon are a possible explanation for hot spots on the IR images from which the corrected profiles taken at different times during the rf pulse and presented in Fig. 8 were derived.

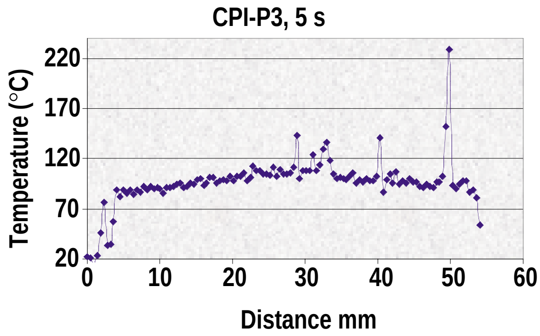

Fig. 6. The uncorrected temperature profile for the CPI-P3 window is extremely flat and this character is preserved after the corrections have been applied.

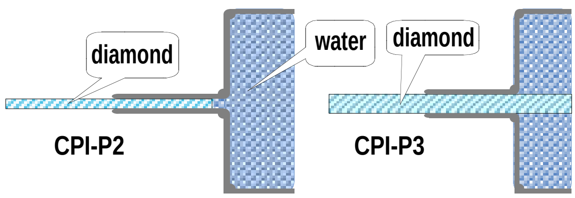

Fig. 7. The window mount designs for CPI-P2 and CPI-P3 are qualitatively different. On the left is CPI-P2's design and on the right is CPI-P3's, which has substantially improved heat transfer characteristics.

4. Conclusion

Two different diamond disks were analyzed using an IR camera. Temperature profiles and maximum temperatures of the windows are in rough agreement with theoretical modeling, but differ significantly in details. The window temperature equilibrates after about 2.5 s at low peak values, which indicates that diamond windows should be able to transmit up to 1 MW rf beams even up to cw operation. Apparent hot spots, which cannot easily be differentiated from regions of high emissivity, do not seem problematic, but need further investigation.

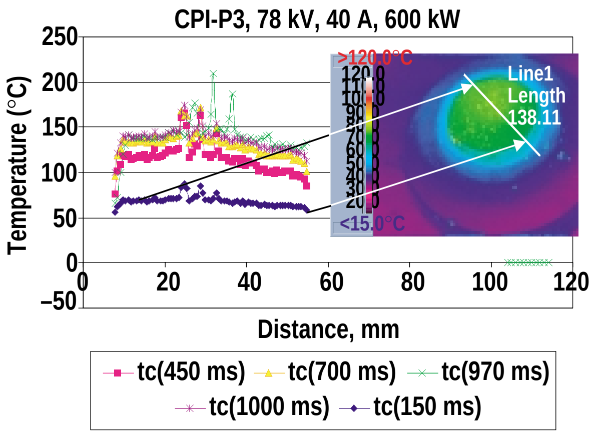

Fig. 8. Hot spots on the CPI-P3 window surface are observed early in the pulse and their infrared signature increases rapidly. Peak apparent temperatures of the hot spots can be up to 100°C higher than the surrounding material.

Acknowledgment

Work supported by U.S. Department of Energy under Contract No. DE-AC03-99ER54463.